

- Szebenyi, D. M. E., Obendorf, S. K., & Moffat, K. (1981) *Nature (London)* 294, 327-332.  
 Takano, T. (1977) *J. Mol. Biol.* 110, 537-568.  
 Tschesche, H. (1977) *Methods Enzymol.* 47 (Part E), 73-84.  
 Williams, R. J. P. (1970) *Q. Rev., Chem. Soc.* 24, 331.

- Williams, T. C., Corson, D. C., & Sykes, B. D. (1984) *J. Am. Chem. Soc.* 106, 5698-5702.  
 Williams, T. C., Corson, D. C., McCubbin, W. D., Oikawa, K., Kay, C. M., & Sykes, B. D. (1986) *Biochemistry* (second paper of three in this issue).

## <sup>1</sup>H NMR Spectroscopic Studies of Calcium-Binding Proteins. 2. Histidine Microenvironments in $\alpha$ - and $\beta$ -Parvalbumins As Determined by Protonation and Laser Photochemically Induced Dynamic Nuclear Polarization Effects<sup>†</sup>

Thomas C. Williams,\* David C. Corson, William D. McCubbin, Kimio Oikawa, Cyril M. Kay, and Brian D. Sykes  
 Medical Research Council of Canada Group in Protein Structure and Function and Department of Biochemistry, University of Alberta, Edmonton, Alberta, Canada T6G 2H7

Received July 18, 1985

**ABSTRACT:** The microenvironments of the histidines in three isoforms of Ca(II)-bound parvalbumin (carp,  $pI = 4.25$ ; pike,  $pI = 5.00$ ; rat,  $pI = 5.50$ ) have been examined with <sup>1</sup>H NMR techniques to probe their protonation characteristics and photochemically induced dynamic nuclear polarizability (photo-CIDNP). The histidine at position 26 (or 25), present in all three of these proteins, shows absolutely *no* photo-CIDNP enhancement of its C<sub>2</sub>H or C<sub>5</sub>H resonances. Nor does this nonpolarizable histidine possess a normal  $pK_a$ ; values range only from 4.20 for carp to 4.32 for pike to 4.44 for rat. The C<sub>2</sub>H and C<sub>5</sub>H resonances of the histidine in this carp isoform split into doublets as the pH is lowered. The magnitude of this splitting depends on the magnetic field strength, temperature, and pH; however, the line intensities within each doublet are temperature-independent. Although the crystal structure of carp parvalbumin indicates that His-26 is exposed to solvent [Kretsinger, R. H., & Nockolds, C. E. (1973) *J. Biol. Chem.* 248, 3313-3326], we conclude that in solution this residue, in its unprotonated state, is part of the hydrophobic core of the protein. In contrast, His-48 in rat parvalbumin and His-106 in pike III parvalbumin show dramatic photo-CIDNP enhancements of their C<sub>2</sub>H, C<sub>5</sub>H, and  $\beta$ -CH<sub>2</sub> <sup>1</sup>H NMR resonances. Combined with its nearly normal  $pK_a$ , 6.14, and exchange-broadened C<sub>2</sub>H resonance, the photo-CIDNP enhancement results for His-48 indicate that its microenvironment differs little from random-coil exposure, consistent with its presumed position on the solvent surface of helix C. However, the protonation behavior of His-106 in pike III suggests that its microenvironment is different from random-coil exposure. Not only is its  $pK_a$  elevated (7.10) and C<sub>2</sub>H resonance minimally broadened, but its C<sub>5</sub>H resonance is also extremely sensitive to protonation/deprotonation of His-25. Because of the mutual sensitivity of the C<sub>5</sub>H resonances of His-25 and His-106 to the protonation/deprotonation of their imidazole rings, we suggest (i) that the protonated form of His-106 is involved in a H bond with a backbone C=O or side-chain -OH in the BC-linker region and (ii) that the protonated form of His-25(26) is expelled from the hydrophobic core. Each of these protonations causes a conformational change in the B-helix/F-helix region. In addition, photo-CIDNP studies of the  $pI = 3.95$  isoform of carp parvalbumin indicate that its single potentially enhanceable residue, Tyr-2, is either buried or involved in H-bond formation via its phenolic -OH group.

Few protein-bound protons have been such useful <sup>1</sup>H NMR<sup>1</sup> spectroscopic probes of intrinsic tertiary structure as have the C<sub>2</sub>H and C<sub>5</sub>H imidazole-ring protons of histidine.<sup>2</sup> Not only are their resonances ordinarily observed as singlets in the relatively uncrowded aromatic region of the <sup>1</sup>H NMR spectrum, but they are also extraordinarily sensitive to pH changes. These attributes, combined with the paucity of histidines in many proteins, facilitate the assignment of resonance pairs (i.e., C<sub>2</sub>H and C<sub>5</sub>H) to specific residues in the amino acid sequence. Spectral perturbations of assigned histidine resonances can then be unequivocally attributed to discrete molecular perturbations in the folded protein (Markley, 1975a).

The microenvironments of individual histidines within a protein have most frequently been assessed by comparisons

of their protonation parameters (e.g.,  $pK_a$ , <sup>1</sup>H  $\rightarrow$  <sup>2</sup>H exchange rates) with those of the free N-acetylated methyl ester or methylamide of histidine (Tanokura et al., 1978; Boschov et al., 1983). In particular, variations in  $pK_a$  have usually been ascribed to the nearness of the imidazole ring to charged, ionizable groups or its participation in H bonding, sluggish

<sup>1</sup> Abbreviations: AB, helix A-loop-helix B region of parvalbumin (residues 7-34); CD, helix C-loop-helix D region of parvalbumin (residues 39-71); EF, helix E-loop-helix F region of parvalbumin (residues 78-108); ED, ethylenediamine; FMN, flavin mononucleotide (riboflavin phosphate); SDS, sodium dodecyl sulfate; D<sub>2</sub>O, deuterium oxide; Tris, tris(hydroxymethyl)aminomethane; Pipes, 1,4-piperazinediethanesulfonic acid; DSS, sodium 4,4-dimethyl-4-silapentane-1-sulfonate; NMR, nuclear magnetic resonance; photo-CIDNP, photochemically induced dynamic nuclear polarization; NOE, nuclear Overhauser effect; UV, ultraviolet; FID, free induction decay.

<sup>2</sup> In accordance with nomenclature recommendations (IUPAC-IUB Joint Commission on Biochemical Nomenclature, 1985), we refer to the imidazole ring protons as C<sub>2</sub>H and C<sub>5</sub>H rather than C<sub>2</sub>H and C<sub>4</sub>H as has been done frequently in the past.

<sup>†</sup> This work was supported by the Medical Research Council of Canada Group in Protein Structure and Function and the Alberta Heritage Foundation for Medical Research (equipment grant for the NT-300WB spectrometer and fellowship and research allowance to T.C.W.).

protonation/deprotonation rates to lack of general-base catalysis, and slowed  $C_2H$   $^1H \rightarrow ^2H$  exchange rates to the inaccessibility of the imidazole ring. In addition, the laser photo-CIDNP (photochemically induced dynamic nuclear polarization) technique has been used to determine the solvent accessibility of histidine residues [for a review, see Kaptein (1980)]. In this method, a codissolved flavin dye is transiently excited to its triplet state by irradiation with laser light. The allylic-like N-H bond of histidine's imidazole ring is particularly susceptible to homolytic cleavage and, if accessible to the dissolved dye, will react with the triplet species to form a transient radical pair. Re-formation of the N-H bond leaves the spin-state equilibrium of the  $C_2H$  and  $C_5H$  protons greatly perturbed, resulting in significant enhancements of their resonance intensities. Because tyrosine and tryptophan are the only other amino acids normally capable of interacting with the triplet-state flavin, this method allows the selective observation of these three residues, greatly simplifying analysis of the  $^1H$  NMR spectrum.

Most parvalbumins have only one histidine in their sequence of 108–109 residues, tyrosine or tryptophan normally being completely absent. Position 26 or its alignment equivalent is occupied by histidine in 10 out of 14 sequenced parvalbumins (Barker et al., 1978). The crystal structure of the  $\beta$ -lineage  $pI = 4.25$  parvalbumin from carp (Kretsinger & Nockolds, 1973) indicates that His-26, located at the start of helix B (and therefore referred to as His B1),<sup>3</sup> is solvent-accessible. Using standard bond lengths and geometries to extrapolate proton positions from these X-ray coordinates, Lee and Sykes (1980, 1982, 1983) determined the solution structure of the EF domain of carp parvalbumin from the paramagnetic shifts induced by Yb(III) in a number of  $^1H$  NMR resonances, including the presumably exposed  $C_2H$  and  $C_5H$  protons of His-26 and the  $CH_3$  protons of the *N*-acetyl group. Williams et al. (1984) have also used the conformational sensitivity of these assigned His-26 resonances to corroborate the preferential displacement of the EF-site Ca(II) ion by the smaller lanthanides [i.e., Yb(III) and Lu(III)]. Aside from a preliminary determination of the  $pK_a$  of His-26 of carp parvalbumin (Lee & Sykes, 1982), none of the common protonation parameters has yet been determined for histidine at position B1, nor has its solvent accessibility been tested by the photo-CIDNP  $^1H$  NMR technique. In addition to His B1, two  $\alpha$ -lineage parvalbumins each have a second histidine residue: rat parvalbumin, at position 48 in helix C (His C9); pike III parvalbumin, at position 106 near the end of helix F (His F9). In order to determine the microenvironments of each of these histidines in the  $Ca_2$  form of parvalbumin, we have studied the protonation behaviors and photo-CIDNP enhanceability of their readily assignable  $^1H$  NMR resonances. The  $pI = 3.95$  isoform of carp parvalbumin lacks even His B1; its sole enhanceable residue, Tyr-2, is exposed to solvent by analogy to Phe-2 of the crystallized  $pI = 4.25$  isoform. We have also tested its accessibility by the photo-CIDNP technique.

## EXPERIMENTAL PROCEDURES

**Materials.** Parvalbumins were isolated from the following sources by the method of Haiech et al. (1979); carp (*Cyprinus*

*carpio*), isoforms  $pI = 3.95$  and  $pI = 4.25$ ; pike (*Esox lucius*), isoform  $pI = 5.0$ ; rat (Sprague-Dawley), isoform  $pI = 5.5$ . The purity of each parvalbumin preparation was verified by amino acid analysis, UV absorption and  $^1H$  NMR spectroscopy, and SDS-polyacrylamide gel electrophoresis.  $D_2O$  (99.8 mol %) was purchased from Bio-Rad. DCl (35% in  $D_2O$ ) and NaOD (40% in  $D_2O$ ) were purchased from Kor Isotopes. DSS was purchased from Merck Sharp & Dohme. FMN and piperazine were purchased from Sigma. KCl (puratronic; metal basis purity) was purchased from Alfa Inorganics.

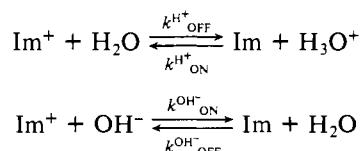
**pH Titrations.** Lyophilized samples of each parvalbumin (10–20 mg) were dissolved separately in 1-mL aliquots of 100 mM KCl/ $D_2O$  at 25 °C and centrifuged. The supernatant was then lyophilized and redissolved in 670  $\mu$ L of  $D_2O$ ; after 10  $\mu$ L each of 50 mM DSS/ $D_2O$ , 150 mM piperazine/ $D_2O$ , and 150 mM ED/ $D_2O$  (pH calibration compounds) was mixed with the protein solution, it was again centrifuged and transferred to a vial with a magnetic stirrer. For the rat and pike parvalbumin pH titrations, a combination microelectrode (Ingold) fitted to a Radiometer PHM60 pH meter was standardized at 40 ( $\pm 0.05$ ) °C with pH 4.00 and 7.00 reference buffers temperature equilibrated by a Lauda circulating water bath. The unadjusted pH of the stirred, temperature-equilibrated protein solution was then determined to an accuracy of  $\pm 0.05$ . Its 300-MHz  $^1H$  NMR spectrum was acquired on a Nicolet Instruments NT-300WB spectrometer thermostated at 40 ( $\pm 0.5$ ) °C. Typical acquisition parameters were as follows: probe size = 5 mm; sample volume = 500  $\mu$ L; protein concentration = 2–4 mM; spectral width =  $\pm 2000$  Hz/16K data points; pulse length = 8  $\mu$ s; preacquisition delay = 100  $\mu$ s; FID filter = Bessel ( $\pm 3000$  Hz) with quadrature phase detection; number of acquisitions = 1000; resolution enhancement = Lorentzian to Gaussian. Additional spectra were acquired under identical conditions after the pH of the protein solution was adjusted in steps of approximately 0.2 pH unit, first downward (from pH 5.5) with 1 M DCl and then upward with 1 M NaOD. The titration of the carp  $pI = 4.25$  isoform was conducted as described above but at 55 °C rather than at 40 °C. Titration of a mixture of 0.5 mM DSS, 2 mM piperazine, 2 mM ED, 2 mM Tris, and 2 mM sodium formate in protein-free 150 mM KCl/ $D_2O$  was also performed at 40 °C in order to determine the pH sensitivities of the chemical shifts of the singlet resonances of these calibration compounds.

The chemical shifts,  $\delta_{obsd}$ , of the  $C_2H$  and  $C_5H$  protons of parvalbumin's histidines were measured as a function of pH;  $pK_a$ 's were then calculated from a four-parameter nonlinear least-squares curve-fitting routine on the basis of the function (Markley, 1975a):

$$\delta_{obsd} = \delta_B + \frac{[H]^n}{([H]^n + K_a^n)} \Delta\delta_{AB}$$

where  $\Delta\delta_{AB}$  is the difference between the chemical shift of the protonated species ( $\delta_A$ ) and the chemical shift of the unprotonated species ( $\delta_B$ ) and  $n$  is the Hill coefficient.

The exchange rates between the unprotonated and protonated forms of parvalbumin's histidines,  $k_{EX}$ , were estimated from the measured increases in their  $C_2H$  line widths at their respective  $pK_a$ 's. For the kinetic scheme that incorporates the effects of general-base/general-acid catalysis on the deprotonation/protonation reactions of the imidazole ring (Ralph & Grunwald, 1969)



<sup>3</sup> To identify the sequence position of a given residue in the structurally homologous parvalbumin series, we have adopted the following notation, developed first for residue identification in myoglobins and hemoglobins: B1 = residue 1 of helix B (His-26 in both carp and rat isoforms; His-25 in pike III); F9 = residue 9 of helix F (His-106 in pike III; Lys-107 in carp; Ala-107 in rat); C9 = residue 9 in helix C (His-48 in rat; Ala-48 in carp; Lys-47 in pike III).

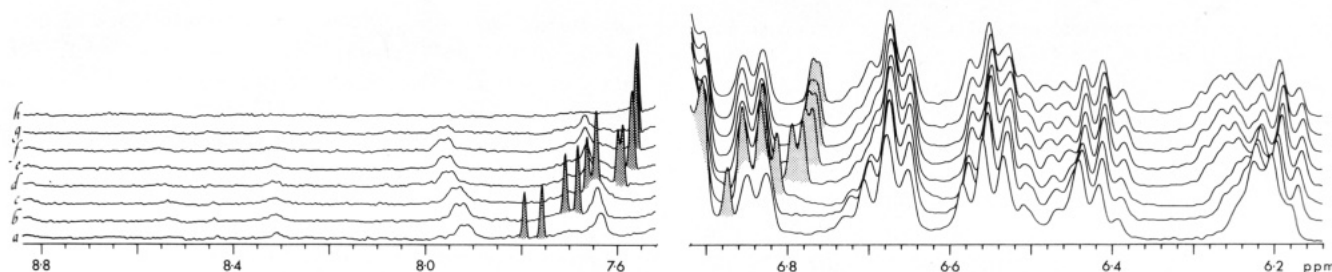


FIGURE 1: 300-MHz  $^1\text{H}$  NMR spectra (8.8–6.2 ppm) of  $pI = 4.25$  carp parvalbumin at selected pH values: a, 4.85; b, 5.20; c, 5.41; d, 5.99; e, 6.52; f, 7.06; g, 8.40; h, 8.91. The  $\text{C}_2\text{H}$  resonances of His-26 are shaded dark gray; its  $\text{C}_5\text{H}$  resonances are shaded light gray. Note also the quartet-like appearance of the meta proton resonance at 6.26 ppm (trace h; tentatively assigned to Phe-29; see text).

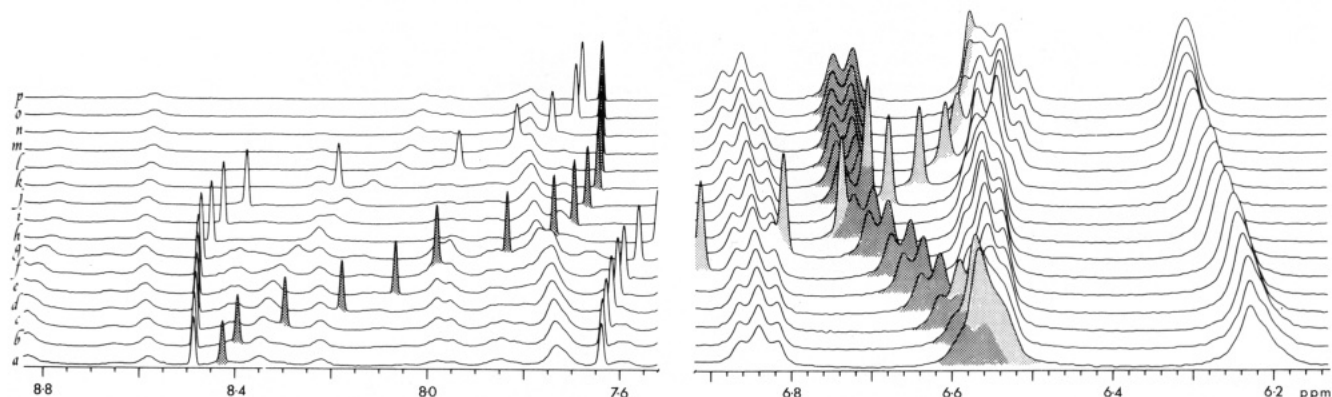


FIGURE 2: 300-MHz  $^1\text{H}$  NMR spectra (8.8–6.2 ppm) of pike III parvalbumin at selected pH values: a, 3.94; b, 4.01; c, 4.17; d, 4.40; e, 4.61; f, 4.80; g, 5.15; h, 5.56; i, 5.84; j, 6.14; k, 6.75; l, 7.35; m, 7.69; n, 8.00; o, 8.41; p, 8.68. The  $\text{C}_2\text{H}$  resonance of His-25 (left-hand side) and the ortho proton resonance of Phe-23 (right-hand side; tentative assignment; see text) are shaded dark gray. The  $\text{C}_5\text{H}$  singlet resonance of His-25 is shaded light gray.

the observed exchange-induced line broadening,  $\Delta\nu_{\text{EX}}$ , is approximated in the fast-exchange limit by

$$\Delta\nu_{\text{EX}} \approx 4\pi(\Delta\delta_{\text{AB}})^2(P_A^2P_B^2)/(P_Ak_{\text{OFF}}^{\text{H}^+} + P_Bk_{\text{OFF}}^{\text{OH}^-})$$

where  $\Delta\delta_{\text{AB}}$  = the difference in the chemical shifts of the acid and base forms of histidine (in Hz),  $P_A$  = the fraction of histidine in its acidic state (i.e., protonated),  $P_B$  = the fraction of histidine in its basic state (i.e., deprotonated), and the rate constants and other variables are as defined above (Piette & Anderson, 1959; Baldo et al., 1975; Sudmeier et al., 1980; Sandstrom, 1982). If, however, one assumes that  $k_{\text{OFF}}^{\text{H}^+} \gg k_{\text{OFF}}^{\text{OH}^-}$  and one measures the line broadening at the  $pK_a$  of the imidazole ring, then the above relation reduces to

$$k_{\text{EX}} \approx \pi(\Delta\delta_{\text{AB}})^2/(4\Delta\nu_{\text{EX}})$$

**NOE Difference Spectra.** A 2.5 mM solution of rat parvalbumin (pH 6.8) was prepared as described above, taking particular precaution to minimize its residual HDO content. A series of six 300-MHz  $^1\text{H}$  NOE difference spectra was collected as pairs of interleaved *on-resonance* irradiation/*off-resonance* irradiation FIDs. The irradiation pulse, centered sequentially on different phenylalanine resonances, was gated *on* for 1 s, followed by a 200- $\mu\text{s}$  delay before FID acquisition. A 10-s delay was allowed between the end of one acquisition and the beginning of the next irradiation pulse. The other acquisition parameters were as described above. The sample temperature was 40  $^\circ\text{C}$ .

**Laser Photo-CIDNP Difference Spectra.** Lyophilized samples of the parvalbumins (50 mg each from carp  $pI = 4.25$ , carp  $pI = 3.95$ , and pike  $pI = 5.0$ ; 20 mg from rat) were dissolved separately in 1.8-mL aliquots of 100 mM KCl/ $\text{D}_2\text{O}$ . The pH of each solution was adjusted to 7.5–8.0 with 1 M NaOD. After centrifugation, the solutions were lyophilized and then redissolved in 1.2 mL of  $\text{D}_2\text{O}$ . Enough 50 mM FMN/ $\text{D}_2\text{O}$  was added to each sample to bring its protein:

FMN ratio to 3–4. Its pH was then readjusted to 7.5–8.0, and the sample was then transferred to a 10-mm flat-bottomed NMR tube. The 270-MHz photo-CIDNP  $^1\text{H}$  NMR spectra were acquired (sample spinning) on a Bruker 270-MHz HXS spectrometer controlled by a Nicolet 1180 data system. For each photo-CIDNP difference spectrum, two FIDs of 20 transients each were collected. In the first, the FIDs were acquired as outlined below, allowing an 11-s delay between transients; in the second, a 1-s irradiation pulse from a Spectra Physics argon gas laser (2.8–3.0 W) was directed through the bottom of the sample by an adjustable shutter-mirror system before the FIDs were acquired, allowing a 10-s delay between transients. The photo-CIDNP  $^1\text{H}$  NMR spectrum was obtained as the difference (*laser on* minus *laser off*) between the Fourier-transformed FIDs. Typical acquisition parameters were as follows: probe size = 10 mm; sample volume = 1.2 mL; protein concentration = 2–4 mM; spectral width =  $\pm 2000$  Hz/16K data points; pulse length = 19  $\mu\text{s}$ ; preacquisition delay = 25  $\mu\text{s}$ ; FID filter = Bessel ( $\pm 3000$  Hz) with quadrature phase detection; number of acquisitions = 20; resolution enhancement = Lorentzian to Gaussian.

## RESULTS

**Protein pH Titrations.** Figures 1–3 illustrate some of the pH-induced changes observed in the aromatic region of the spectra of carp parvalbumin ( $pI = 4.25$ ), pike parvalbumin ( $pI = 5.0$ ), and rat parvalbumin ( $pI = 5.5$ ), respectively. In Figure 4, the titration curves of the  $\text{C}_2\text{H}$  and  $\text{C}_5\text{H}$  histidine protons from all three parvalbumins species are displayed as overlay plots.

(A) **Carp Parvalbumin ( $pI = 4.25$ ).** There are three significant features to note in this series of spectra (Figure 1). Not only did the  $\text{C}_2\text{H}$  resonance (shaded dark gray) and  $\text{C}_5\text{H}$  resonance (shaded light gray) of His-26 move downfield as the pH was lowered, each split into two singlets; at lower pH,

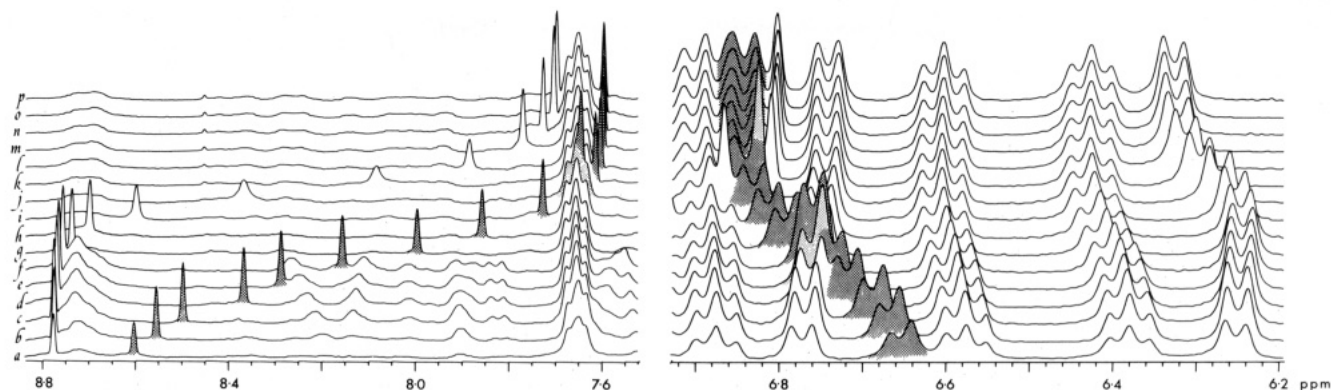


FIGURE 3: 300-MHz  $^1\text{H}$  NMR spectra (8.8–6.2 ppm) of rat parvalbumin at selected pH values: a, 3.72; b, 3.83; c, 3.96; d, 4.16; e, 4.29; f, 4.52; g, 4.79; h, 5.07; i, 5.46; j, 5.92; k, 6.40; l, 6.83; m, 7.28; n, 7.65; o, 8.10; p, 8.40. The  $\text{C}_2\text{H}$  resonance of His-26 (left-hand side) and the ortho proton resonance of Phe-24 (right-hand side; tentative assignment; see text) are shaded dark gray.

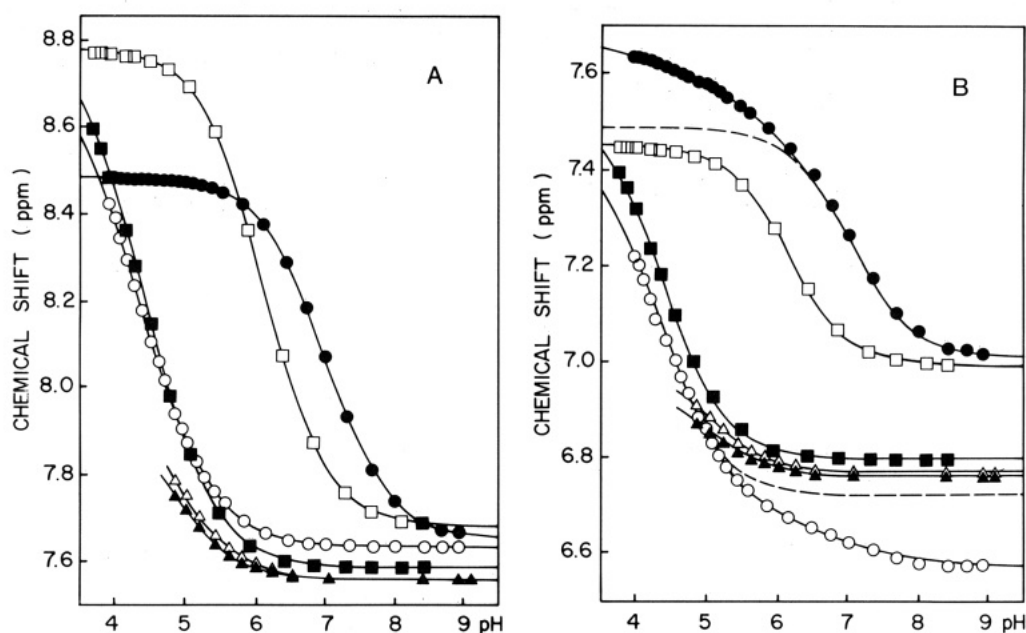


FIGURE 4: Plot of the chemical shifts of histidine  $\text{C}_2\text{H}$  (A) and  $\text{C}_5\text{H}$  protons (B) vs. pH: His-26, carp parvalbumin ( $\Delta$ ;  $\blacktriangle$ ); His-26, rat parvalbumin ( $\blacksquare$ ); His-48, rat parvalbumin ( $\square$ ); His-25, pike parvalbumin ( $\circ$ ); His-106, pike parvalbumin ( $\bullet$ ). The dashed lines in part B represent the calculated curves for the pike  $\text{C}_5\text{H}$  resonances in the absence of His-25/His-106 interactions.

Table I: Protonation Parameters for the  $\text{C}_2\text{H}$  Resonances of Histidines in Parvalbumins<sup>a</sup>

histidine	$\delta_A$ (ppm)	$\delta_B$ (ppm)	$\Delta\delta_{AB}$ (ppm)	$\Delta\nu_{EX}$ (Hz)	$n$	$\text{pK}_a$	$k_{EX} (\times 10^{-4} \text{ s}^{-1})$
His B1							
carp (upfield)	8.833	7.559	1.274		1.000	4.35	
carp (downfield)	8.833	7.560	1.273		1.000	4.20	
pike	8.601 (0.013)	7.644 (0.003)	0.957	0.4	1.000	4.525 (0.016)	16
	8.805 (0.031)	7.636 (0.002)	1.169	0.4	0.816 (0.020)	4.320 (0.030)	24
rat	8.753 (0.013)	7.595 (0.004)	1.158	0.5	1.000	4.486 (0.017)	19
	8.860 (0.019)	7.587 (0.002)	1.273	0.5	0.868 (0.018)	4.393 (0.018)	23
His C9							
rat	8.775 (0.001)	7.688 (0.001)	1.087	5.2	1.000	6.144 (0.003)	1.6
His F9							
pike	8.481 (0.001)	7.665 (0.003)	0.816	1.0	1.000	7.009 (0.007)	4.7
	8.484 (0.001)	7.655 (0.002)	0.829	1.0	0.937 (0.007)	7.020 (0.004)	4.9

<sup>a</sup> Values in parentheses are standard deviations.

the separation in the  $\text{C}_2\text{H}$  and  $\text{C}_5\text{H}$  singlet resonances increased. This doubling of resonances was not limited to the imidazole ring protons; the resonance of the meta protons of one phenylalanine residue [assigned to Phe-29 by Levine et al. (1982)] and the para proton resonance of another phenylalanine [5.56 ppm, not shown; assigned to Phe-24 by Levine et al. (1982)] were each observed as a quartet-like doublet of triplets. Such selective doubling of the resonances of these B-helix residues may indicate that the side chains of Phe-24, His-26, and Phe-29 experience slow exchange between two

marginally different conformations or that this preparation of carp parvalbumin was an irresolvable mixture of isoforms. Although severe precipitation of this carp protein prevented data collection below pH 4.8, the total protonation-induced chemical shift changes for the two His-26  $\text{C}_2\text{H}$  resonances were estimated as described above (see Table I). The  $\text{pK}_a$ 's of His-26 in these two forms of parvalbumin were estimated as 4.20 and 4.35 from the total protonation-induced chemical shift changes of the  $\text{C}_2\text{H}$  resonances of His-25 and His-26 of pike III and rat parvalbumins, respectively.

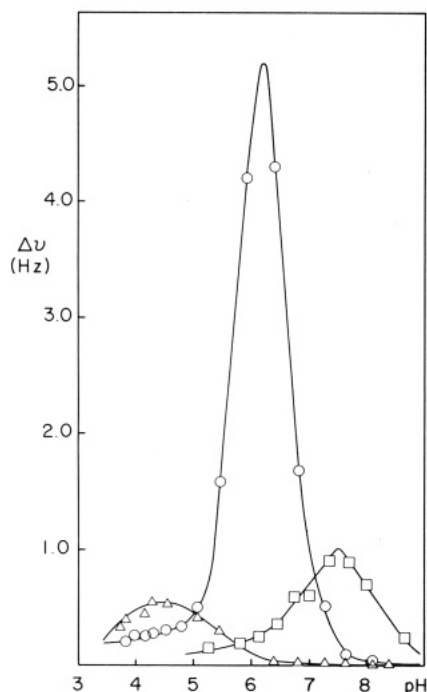


FIGURE 5: Plot of the exchange broadening contribution to the line width of the histidine  $C_2H$  resonance vs. pH: His-26, rat parvalbumin ( $\Delta$ ); His-48, rat parvalbumin (O); His-106, pike parvalbumin ( $\square$ ).

(B) *Pike Parvalbumin* ( $pI = 5.0$ ). The difference in the titration behaviors of pike parvalbumin's histidines, His-25 and His-106, was immediately apparent from the pH dependence of its  $C_2H$  resonances (Figure 2). Although the singlet resonance at 7.66 ppm (dark gray, trace p) did not split into two as the pH was lowered, the plot of its pH-dependent chemical shift (Figure 4A) yielded a  $pK_a$  of 4.32, nearly identical with that of His-26 of the carp isoform (Table I); it was therefore assigned to the  $C_2H$  proton of His-25. Analysis of the pH dependence of the chemical shift of the  $C_2H$  resonance at 7.69 ppm indicated that the  $pK_a$  of His-106 was 7.01 (Figure 4A; Table I). The increases in line width of the  $C_2H$  resonances of His-25 and His-106 of pike parvalbumin are plotted as a function of pH in Figure 5. From the increase in line width at the  $pK_a$  of His-106 (1 Hz), the exchange rate between its protonated and unprotonated forms was estimated to be  $4.8 \times 10^4 \text{ s}^{-1}$ . Similarly, the small increase in line width (approximately 0.4 Hz) of the  $C_2H$  resonance of His-25 was used to calculate an exchange rate of  $20 \times 10^4 \text{ s}^{-1}$  for His-25 between its protonated and unprotonated forms. Note that the titration behaviors of both histidine  $C_2H$  resonances are well-fitted by simple one-proton models with a Hill coefficient,  $n$ , equal to 1. Contrast this to the interesting behaviors of the  $C_5H$  resonances of His-25 and His-106; during protonation/deprotonation of the other, each deviates sharply from a titration behavior calculated from the simple model used for analysis of the  $C_2H$  resonances (Figure 4B). The deviation of the  $C_5H$  resonance of protonated His-106 is attributed to fast exchange between two conformations of the protein, one in which His-25 is protonated and the other in which it is not. Similarly, the deviation of the  $C_5H$  resonance of unprotonated His-25 is attributed to fast exchange between a different set of two conformations of the protein, one in which His-106 is protonated and the other in which it is not. The greater solubility of pike parvalbumin at low pH allowed data collection to continue to about pH 3.8. In so doing, the sensitivity of the doublet Phe resonance at 6.735 ppm (trace p, Figure 2; dark gray) to protonation of His-25 was revealed. Its

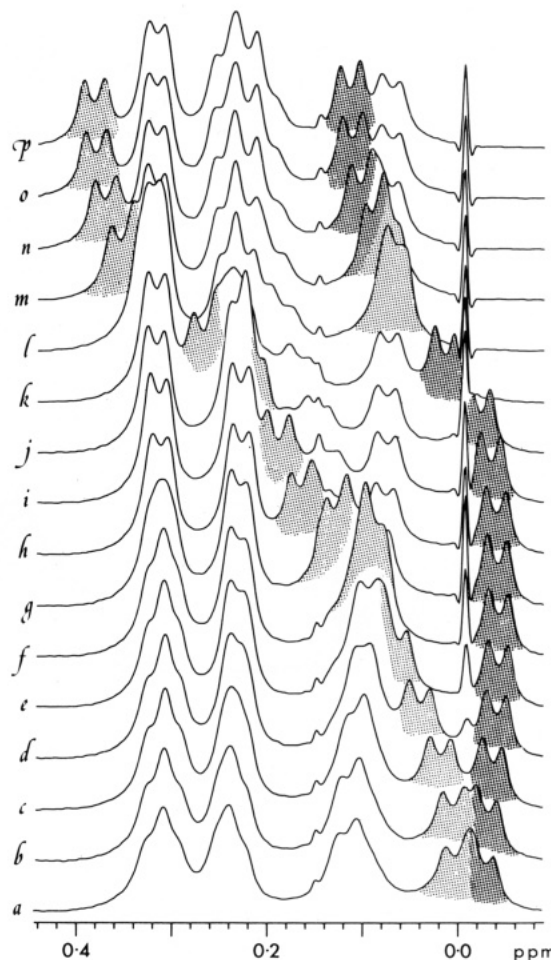


FIGURE 6: 300-MHz  $^1H$  NMR spectra (0.4 to  $-0.1$  ppm) of pike III parvalbumin vs. pH: the pH values of traces a–p are the same as those for Figure 2. The shaded resonances were assigned to the methyl protons of Val-105 (see text).

chemical shift, relative integrated intensity (2 protons), and multiplet pattern label this doublet as a phenylalanine ortho proton resonance; as judged from their apparent proximities to histidine-26 in the crystal structure of carp parvalbumin, Phe-24, Phe-29, Phe-30, and Phe-85 are candidates for the assignment of the pH-sensitive doublet resonance. The two methyl doublet resonances of Val-105 have also been tentatively assigned. The marked sensitivity of the doublet resonances at 0.39 and 0.12 ppm (Figure 6, trace p) to protonation of His-106 was used to assign the resonance at 0.39 ppm to the  $\gamma$ -1 methyl group of Val-105 and the resonance at 0.12 ppm to the  $\gamma$ -2 methyl group of Val-105 (Parello et al., 1974; Lee & Sykes, 1983; Corson et al., 1986).

(C) *Rat Parvalbumin* ( $pI = 5.5$ ). As illustrated in Figures 3 and 4A, the  $C_2H$  resonances of rat parvalbumin's two histidines were readily differentiated by their dissimilar pH titration behaviors. The singlet resonance at 7.61 ppm (Figure 3, trace p; dark gray) was assigned to His-26 on the basis of its  $pK_a$  and other protonation parameters listed in Table I. Not only did this resonance have the abnormally low  $pK_a$  (4.2–4.5) and narrow line width characteristic of the carp His-26 and pike His-25 resonances, but its chemical shift in both its acidic and basic forms also closely matched those of the aforementioned analogues. The protonation exchange rate of His-26 was calculated from its line broadening as described above; its value,  $(19\text{--}23) \times 10^4 \text{ s}^{-1}$ , is nearly identical with the exchange rate calculated for His-25 of the pike III isoform. By obvious elimination, the singlet resonance at 7.71 ppm (Figure



3, trace p) was therefore assigned to the C<sub>2</sub>H proton of His-48. However, its calculated pK<sub>a</sub> (6.14) and exchange-broadened line width implied a microenvironment different from that of histidines at position B1 or F9. Several well-resolved, upfield-shifted aromatic resonances of rat parvalbumin also sensed the titration of one or the other of its histidine residues. The doublet at 6.85 ppm (Figure 3, trace p; dark gray) shifted upfield during protonation of His-26; this behavior, quite like the His-25 protonation-induced shifting of the doublet resonance at 6.735 ppm in the spectrum of pike III parvalbumin, suggested that the resonances at 6.85 and 6.735 ppm in the spectra of rat and pike III parvalbumins, respectively, arise from the same phenylalanine residue. Of the four potential assignments mentioned above, only Phe-24, Phe-29, and Phe-30 are conserved in the amino acid sequence of rat parvalbumin; Phe-85 was therefore eliminated as a possible assignment. From the NOE experiments described below, this doublet ortho proton resonance was assigned to that Phe residue whose para proton resonance falls at 5.56 ppm. As indicated above, Levine et al. (1982), on the basis of calculated ring-current shifts (Parello et al., 1974), have assigned this most upfield-shifted para proton triplet to Phe-24. We therefore have tentatively assigned this low pH sensitive ortho proton doublet to Phe-24 in rat parvalbumin and to Phe-23 in pike parvalbumin. Although our failure to titrate the carp pI = 4.25 isoform below pH 4.8 prohibited the full observation of the analogous protonation-induced shift, the doublet resonance at 6.84 ppm in the spectrum of carp parvalbumin (Figure 1, trace h) showed the beginning of an induced upfield shift at the low pH extreme. For this reason, we also assign the 6.84 ppm resonance in the carp spectrum to Phe-24 [note: this is contrary to the assignment of this resonance to Phe-85 made by Levine et al. (1982)]. The doublet resonance at 6.33 ppm in the spectrum of rat parvalbumin (Figure 3, trace p) also showed pH sensitivity. Unlike the resonance at 6.85 ppm, however, the resonance at 6.33 ppm was considerably more sensitive to protonation of His-48 than to protonation of His-26. Because there are no phenylalanine residues near His-48 except Phe-47 (as indicated by the crystal structure of the carp protein), we have assigned the doublet resonance at 6.33 ppm to the ortho protons of Phe-47.

**NOE Experiments.** The homonuclear Overhauser effects from the series of six phenylalanine resonance NOE experiments are shown as difference spectra in Figure 7. To illustrate the spin connectivities in the well-resolved aromatic region, a normal (nonirradiated) spectrum is displayed in register. Within each difference spectrum (*nonirradiated* minus *irradiated*), the most intense multiplet arises from the irradiated resonance and appears as a "positive" peak (shaded light gray); the other, smaller positive multiplets (negative enhancements) arise from ring protons within the same phenylalanine residue. Spectra a, c, and e show the connectivities between the ortho/meta, ortho/meta/para, and meta/para protons of one phenylalanine residue (Phe B); spectra b and f show the connectivities between the ortho/meta/para and meta/para protons of a second phenylalanine residue (Phe A). The connectivity between the meta protons of Phe-47 and the ortho protons of Phe-47 (the resonance at 6.33 ppm having been assigned as described above) is shown in d. The pattern of two upfield-shifted para proton triplet resonances (at 5.79 and 6.0, ppm in the spectrum above) is characteristic of many parvalbumins. The farthest upfield-shifted para resonance in the spectrum of carp parvalbumin (pI = 4.25) has been assigned to Phe-24 by Levine et al. (1982) as already mentioned; similarly, the other resolved para resonance has been assigned

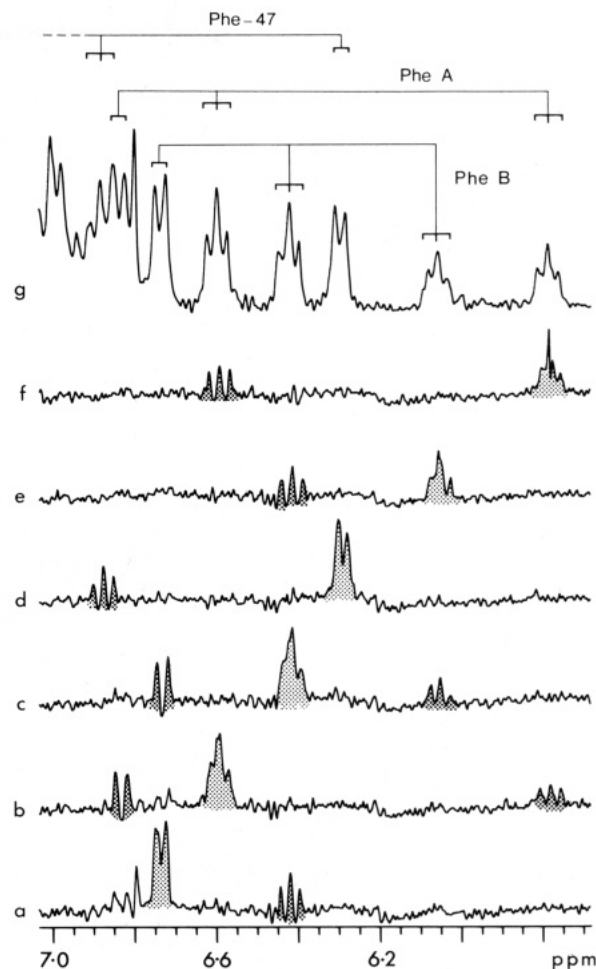


FIGURE 7: 300-MHz <sup>1</sup>H NMR NOE-difference spectra: rat parvalbumin (pH 6.8, 40 °C), phenylalanine resonances. Resonances shaded light gray were preirradiated for 1 s prior to data acquisition; resonances shaded dark gray represent the resultant negative NOEs. The unperturbed spectrum is shown in trace g. NOE-deduced spin connectivities are indicated by the overlying brackets, together with the tentative assignments to individual Phe residues.

to Phe-29. Because the ordered connectivities for the Phe A and Phe B resonances determined by these NOE experiments qualitatively match the scalar-coupling connectivities determined in the previous assignment studies, the Phe A resonances are assigned to residue 24 and the Phe B resonances are assigned to residue 29.

**Histidine C<sub>2</sub>H Doublets.** Although the C<sub>2</sub>H proton resonance of a histidine residue is normally observed as a singlet, long-range scalar coupling to the C<sub>5</sub>H imidazole ring proton (approximately 1.6 Hz; Wider et al., 1981) may be observed if spectrometer resolution and natural line width permit. Throughout most of their titrations, the C<sub>2</sub>H resonances of His-106 (pike III) and His-48 (rat) did indeed appear as doublets. These doublet splittings (0.9 Hz for the pike III isoform; 1.2 Hz for the rat isoform), however, remained constant as the pH was varied and were attributed to long-range scalar coupling to the C<sub>5</sub>H proton.

However, the doublet character of the C<sub>2</sub>H resonance of His-26 in carp parvalbumin was unique. The separation of lines (in Hz) within this doublet varied as a function of magnetic field strength (not shown), pH, and temperature, being greatest (approximately 11 Hz at 55 °C) at pH 4.85. In addition, the doublet splitting of the C<sub>5</sub>H resonance did not match that of the C<sub>2</sub>H resonance, being approximately 9 Hz at this low-pH limit. The source of this splitting, therefore, was *not* scalar coupling. Increase in temperature had no effect

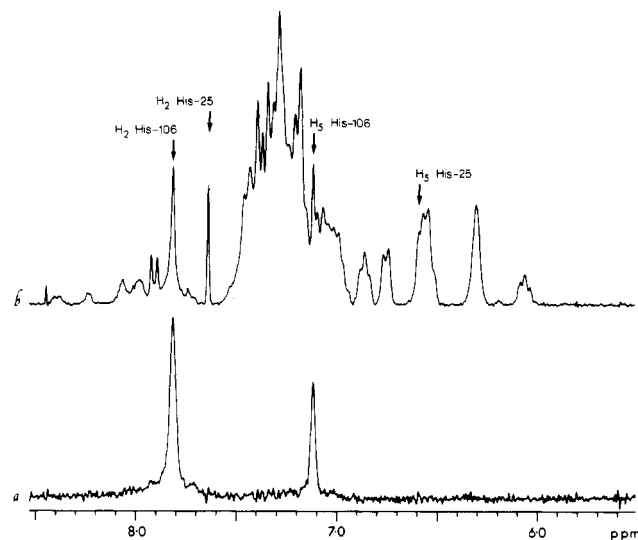


FIGURE 8: 270-MHz  $^1\text{H}$  NMR laser photo-CIDNP difference spectrum of pike III parvalbumin: a, light minus dark difference spectrum; b, dark spectrum. Sample conditions: 4 mM parvalbumin, pH 7.7, 150 mM KCl, 1 mM FMN, and 40  $^\circ\text{C}$ .

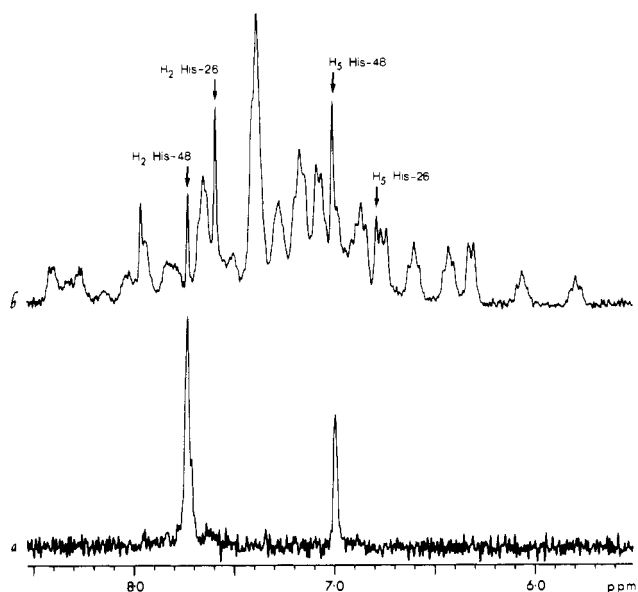


FIGURE 9: 270-MHz  $^1\text{H}$  NMR laser photo-CIDNP difference spectrum of rat parvalbumin: a, light minus dark difference spectrum; b, dark spectrum. Sample conditions: 2 mM parvalbumin, pH 7.7, 150 mM KCl, 0.5 mM FMN, and 40  $^\circ\text{C}$ .

on the intensity ratio of the lines of the doublet.

**Laser Photo-CIDNP Experiments.** All of the photo-CIDNP experiments presented in this paper were conducted at slightly alkaline pH (7.5–8.0); conclusions drawn of the accessibility of a given residue *do not* account for possible pH-dependent changes in conformation. However, the results clearly corroborated the unique microenvironment of His B1. The two resonances assigned to the  $\text{C}_2\text{H}$  and  $\text{C}_5\text{H}$  protons of His-26 in carp parvalbumin showed *no* photo-CIDNP enhancement. Similar results are shown in Figures 8 and 9 where the resonances assigned to His-25 (pike III) and His-26 (rat) also remained unenhanced. These results indicate either that the imidazole ring of His B1 is inaccessible to the flavin molecule or that abstraction of an NH imidazole proton is prohibited, possibly by its involvement as a proton donor in a H bond.

The photo-CIDNP behaviors of His-106 (pike III) and His-48 (rat) strongly contrasted the results for His B1. Dramatic enhancements of the  $\text{C}_2\text{H}$  and  $\text{C}_5\text{H}$  proton reso-

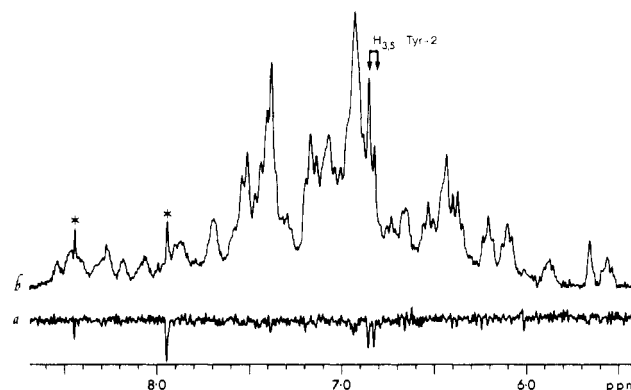


FIGURE 10: 270-MHz  $^1\text{H}$  NMR laser photo-CIDNP difference spectrum of  $p\text{I} = 3.95$  carp parvalbumin: a, light minus dark difference spectrum; b, dark spectrum. Sample conditions: 4 mM parvalbumin, pH 7.7, 150 mM KCl, 1 mM FMN, and 40  $^\circ\text{C}$ .

nances of His-106 (Figure 8) clearly indicated that the dye was allowed free access to its imidazole ring in the unprotonated state. Likewise, enhancement of both proton resonances of His-48's imidazole ring proved its accessibility (Figure 9). Note also that the  $p\text{I} = 3.95$  isoform of carp parvalbumin, having neither histidines nor tryptophans, gave only a very weak negative enhancement (emission) from its single tyrosine residue (Figure 10). Normally, an accessible protein-bound tyrosine will yield a strong doublet emission from its 3,5-ring protons and a weaker doublet emission from its 2,6 protons. The failure to yield the expected strong photo-CIDNP enhancements from its ring protons suggested that Tyr-2 is *not* as accessible to solvent as is indicated by the position of the analogous Phe residue in the crystal structure of the  $p\text{I} = 4.25$  isoform. This observation is consistent with the  $^{13}\text{C}$  NMR study of this isoform (Nelson et al., 1976), which showed Tyr-2 to be immobile in the  $\text{Ca(II)}$  form of the protein.

## DISCUSSION

**Microenvironment of His B1.** Parvalbumin's highly conserved histidine (at position 1 of helix B; residue 26 in most isoforms) occupies a remarkably unique microenvironment. Its extraordinarily low  $pK_a$  (4.20–4.50) in the metal-bound forms of the protein indicates a marked preference for its unprotonated state. In addition, its inability to interact with codissolved flavin and generate photo-CIDNP enhancements suggests that its location within the folded protein is relatively restricted. Extremely slow hydrogen  $\rightarrow$  deuterium exchange at its  $\text{C}_2\text{H}$  ring position (T. Williams, D. C. Corson, & B. D. Sykes, unpublished results) lends further support to the apparent concealment of the imidazole portion of His B1 in parvalbumin isoforms.

Such histidine characterizations, though uncommon, are not unprecedented. Several highly conserved histidine residues in a variety of proteins also titrate with abnormally low  $pK_a$ 's. In myoglobins, His B5 (residue 24 in most species) was assigned a  $pK_a$  of 4.5 in the cyano complex and His GH1 (residue 119) a  $pK_a$  between 5.5 and 5.6, regardless of its liganded state (Carver & Bradbury, 1984); their low  $pK_a$ 's have been attributed in part to H-bond formation between His B5 and His GH1 (Takano, 1977). Another  $pK_a$  in the range 5.1–5.6 has been assigned to one of the heme-cavity histidines in myoglobin, His E7 (residue 58, 61, or 64, depending on the species), which is H-bonded to the sixth iron ligand on the distal side of the heme (Mabbutt et al., 1983), or His FG2, which is involved in a  $\pi$ - $\pi$  interaction with the porphyrin ring (Krisnamoorthi & La Mar, 1984). In chymotrypsinogen,

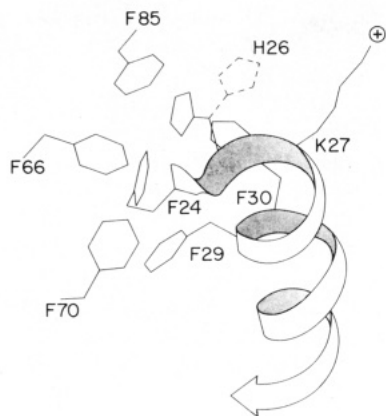


FIGURE 11: Ribbon drawing of the proposed reorientation of His B1 in the hydrophobic core of parvalbumin (derived from the X-ray coordinates of  $pI = 4.25$  carp parvalbumin; Moews & Kretsinger, 1975). The dashed line represents the X-ray-determined position of His-26's side chain; the solid line represents its proposed core orientation.

His-40 titrates with a  $pK_a$  of 4.6 due to H-bond formation with nearby Asp-194 (Markley & Ibanez, 1978). In the postsynaptic neurotoxins of snake venoms, His-21 (of toxin B) and His-22 (of  $\alpha$ -cobratoxin) have a  $pK_a$  of 4.6–4.9 (Endo et al., 1982; Hider et al., 1982); His-6, found in erabutoxins a, b, and c, titrates with a  $pK_a < 3$  and is apparently protonated only when the protein denatures (Inagaki et al., 1978). A low  $pK_a$  is not necessarily synonymous with the inaccessibility of a histidine, ribonuclease A's hidden His-48 having an apparently normal  $pK_a$  of 6.3 (Markley, 1975b). However, failure to generate photo-CIDNP enhancements has corroborated the inaccessibility of a number of low  $pK_a$  histidines, the above-mentioned residues of the neurotoxins being most notable (Muszkat et al., 1984).

The doublet splitting of the  $C_2H$  and  $C_5H$  resonances of His-26 in the  $\beta$ -parvalbumin from carp shows extraordinarily well the unusual microenvironment of this residue. Staphylococcal nuclease (Markley et al., 1970), neurophysin II (Cohen et al., 1972), soybean trypsin inhibitor (Markley, 1973), and dihydrofolate reductase (Gronenborn et al., 1981a,b; Birdsall et al., 1984) all possess histidines whose resonances appear as doublets, their separation being most pronounced at the midpoint of the difference in their  $pK_a$ 's. Markley (1975a), Gronenborn et al. (1981a,b), and Birdsall et al. (1984) have attributed such doublet character to slow exchange between two conformations of the protein, each of the forms having a different  $pK_a$  for a given histidine residue. Of those parvalbumins studied thus far, only the isoform from carp has shown this peculiar resonance pairing. Because the other isoforms also lack Phe-85 (as do most  $\alpha$ -lineage parvalbumins), we suggest that doubling of the His-26 and Phe-24 resonances arises from slow exchange between two conformations that differ in the orientations of these affected residues relative to Phe-85, the contribution from its ring current causing slightly different secondary shifts, or that the parvalbumin preparation was microheterogeneous, two isoforms of identical  $pI$  being present in nearly equal amounts. Although the two  $C_2H$  resonances of His-26 converge at neutral pH and high temperature (55 °C), the  $C_5H$  resonances of the two uncharged histidine forms remain resolved. This indicates that the difference in environments of these histidines within the protein is greater for position 5 of the imidazole ring than it is for position 2 and that the exchange rate is slow ( $< 2 \text{ s}^{-1}$ ).

We propose that the uncharged imidazole ring of His B1 in parvalbumin is an integral residue of its hydrophobic core

(Figure 11). The observed fast exchange of His B1 between its unprotonated and its protonated forms would also suggest that expulsion from the hydrophobic core is coupled to a restricted, but rapid, conformational change. Such a conformational change is *not* expected to significantly alter the secondary structure of helix B, model helical structures remaining intact upon protonation of histidine's side chain (Sueki et al., 1984). The preference of histidine for the interior regions of a protein has been predicted from statistical analyses of this residue's occurrence in X-ray-determined structures of many globular proteins (Nagano & Ponnuswamy, 1984; Prabhakaran, 1984). That His B1 is so highly conserved in parvalbumins may be related to the significantly smaller volume of its side-chain ring compared to that of phenylalanine: the contribution of histidine's amino acid side chain toward its partial molal volume is  $55.1 \text{ cm}^3 \cdot \text{mol}^{-1}$ , whereas phenylalanine's contribution is  $79.0 \text{ cm}^3 \cdot \text{mol}^{-1}$ , an increase of nearly 44% (Mishra & Ahluwala, 1984).

**Microenvironment of His F9.** Only the pike III protein has histidine in this position of the amino acid sequence; the parvalbumins from most  $\beta$ -lineage sources have lysine instead. Three important observations were made concerning this residue. First, its  $pK_a$  is 0.6–0.9 pH unit higher than that of comparable analogues of solvent-exposed noninteracting histidine; second, in its unprotonated state, His F9 is exposed to solvent as deduced from its photo-CIDNP enhancements; and third, the  $^1\text{H}$  NMR resonances of its imidazole ring protons are quite sensitive to protonation of His B1. We conclude from these observations that (i) His F9, in its protonated state, is involved as a proton donor in H-bond formation with a residue in the linker region between helices B and C and (ii) upon expulsion of protonated His B1 from the hydrophobic core His F9 experiences a moderate change in conformation, presumably associated with an adjustment of the helix B–helix F contacts.

**Microenvironment of His C9.** Of all the parvalbumins yet sequenced, only the  $\alpha$ -isoform from rat skeletal muscle has histidine at position C9. His-48 appears to be the most solvent accessible, noninteracting histidine of the three examined in this study. Its  $pK_a$ ,  $k_{\text{EX}}$ , and  $C_2H/C_5H$   $^1\text{H}$  NMR chemical shifts are very like those of simple histidine analogues. The positive photo-CIDNP effects strongly corroborate its solvent exposure at physiological pH. In contrast to the consequences of protonation of His B1 or deprotonation of His F9, His C9's protonation parameters indicate *no* significant conformational change associated with the protonation/deprotonation reactions of its imidazole ring.

#### ACKNOWLEDGMENTS

We thank Glen Bigam for the 400-MHz  $^1\text{H}$  NMR spectra of carp parvalbumin that showed the field-dependent splitting of its His-26 resonances and Dr. J.-R. Brisson for developing the computer program used to evaluate the pH titration data.

**Registry No.** L-His, 71-00-1; L-Tyr, 60-18-4.

#### REFERENCES

- Baldo, J. H., Halford, S. E., Patt, S. L., & Sykes, B. D. (1975) *Biochemistry* 14, 1893–1899.
- Barker, W. C., Ketcham, L. K., & Dayhoff, M. D. (1978) in *Atlas of Protein Sequence and Structure* (Dayhoff, M. D., Ed.) pp 273–283, National Biomedical Research Foundation, Washington, DC.
- Birdsall, B., Bevan, A. W., Pascual, C., Roberts, G. C. K., Feeney, J., Gronenborn, A., & Clore, G. M. (1984) *Biochemistry* 23, 4733–4742.



- Boschcov, P., Seidel, W., Muradian, J., Tominaga, M., Paiva, A. C. M., & Juliano, L. (1983) *Bioorg. Chem.* 12, 34-44.
- Carver, J. A., & Bradbury, J. G. (1984) *Biochemistry* 23, 4890-4905.
- Cohen, P., Griffin, J. H., Camier, M., Caizergues, M., & Fromageot, P. (1972) *FEBS Lett.* 25, 282-286.
- Corson, D. C., Williams, T. C., Kay, L. E., & Sykes, B. D. (1986) *Biochemistry* (first paper of three in this issue).
- Endo, T., Inagaki, F., Hayashi, K., & Miyazawa, T. (1982) *Eur. J. Biochem.* 122, 541-547.
- Gronenborn, A., Birdsall, B., Hyde, E. I., Roberts, G. C. K., Feeney, J., & Burgen, A. S. V. (1981a) *Nature (London)* 290, 273-274.
- Gronenborn, A., Birdsall, B., Hyde, E. I., Roberts, G. C. K., Feeney, J., & Burgen, A. S. V. (1981b) *Mol. Pharmacol.* 20, 145-153.
- Haiech, J., Derancourt, J., Pechère, J.-F., & Demaille, J. G. (1979) *Biochimie* 61, 583-587.
- Hider, R. C., Drake, A. F., Inagaki, F., Williams, R. J. P., Endo, T., & Miyazawa, T. (1982) *J. Mol. Biol.* 158, 275-291.
- Inagaki, F., Miyazawa, T., Hori, H., & Tamiya, N. (1978) *Eur. J. Biochem.* 89, 433-442.
- IUPAC-IUB Joint Commission on Biochemical Nomenclature (1985) *J. Biol. Chem.* 260, 14-42.
- Kaptein, R. (1980) in *Biological Magnetic Resonance* (Berliner, L. J., & Reuben, J., Eds.) Vol. 4, Chapter 3, Plenum, New York.
- Kretsinger, R. H., & Nockolds, C. E. (1973) *J. Biol. Chem.* 248, 3313-3326.
- Krishnamoorthi, R., & La Mar, G. N. (1984) *Eur. J. Biochem.* 138, 135-140.
- Lee, L., & Sykes, B. D. (1980) *Adv. Inorg. Biochem.* 2, 183-210.
- Lee, L., & Sykes, B. D. (1982) in *Biochemical Structure Determination by NMR* (Bothner-By, A. A., Glickson, J. D., & Sykes, B. D., Eds.) pp 169-188, Marcel Dekker, New York.
- Lee, L., & Sykes, B. D. (1983) *Biochemistry* 22, 4366-4373.
- Levine, B. A., Dalgarno, P. C., Esnouf, M. P., Klevitt, R. E., Scott, G. M. M., & Williams, R. J. P. (1982) in *Mobility and Function in Proteins and Nucleic Acids*, pp 72-97, Pitman, London.
- Mabbutt, B. C., Appleby, C. A., & Wright, P. E. (1983) *Biochim. Biophys. Acta* 749, 281-288.
- Markley, J. L. (1973) *Biochemistry* 12, 2245-2249.
- Markley, J. L. (1975a) *Acc. Chem. Res.* 8, 70-80.
- Markley, J. L. (1975b) *Biochemistry* 14, 3546-3554.
- Markley, J. L., & Ibanez, I. B. (1978) *Biochemistry* 17, 4627-4640.
- Markley, J. L., Williams, M. N., & Jardetzky, O. (1970) *Proc. Natl. Acad. Sci. U.S.A.* 65, 645-651.
- Mishia, A. K., & Ahluwalia, J. C. (1984) *J. Phys. Chem.* 88, 86-92.
- Muszkat, K. A., Khait, I., Hayashi, K., & Tamiya, N. (1984) *Biochemistry* 23, 4913-4920.
- Nagano, K., & Ponnuswamy, P. K. (1984) *Adv. Biophys.* 18, 115-148.
- Nelson, D. J., Opella, S. J., & Jardetzky, O. (1976) *Biochemistry* 15, 5552-5560.
- Parello, J., Cavé, A., Puigdomenech, P., Maury, C., Capony, J. P., & Pechère, J.-F. (1974) *Biochimie* 56, 61-76.
- Piette, L. H., & Anderson, W. A. (1959) *J. Chem. Phys.* 30, 899.
- Prabhakaran, M. (1984) *J. Theor. Biol.* 106, 25-40.
- Ralph, E. K., & Grunwald, E. (1969) *J. Am. Chem. Soc.* 91, 2422-2425.
- Sandstrom, J. (1982) in *Dynamic NMR Spectroscopy*, Chapter 6, Academic Press, London.
- Sudmeier, J. L., Evelhoch, J. L., & Jonsson, N. B. H. (1980) *J. Magn. Reson.* 40, 377-390.
- Sueki, M., Lee, S., Powers, S. P., Denton, J. B., Konishi, Y., & Scheraga, H. A. (1984) *Macromolecules* 17, 148-155.
- Takano, T. (1977) *J. Mol. Biol.* 110, 537-568.
- Tanokura, M., Tasumi, M., & Miyazawa, T. (1978) *Chem. Lett.*, 737-742.
- Wider, G., Baumann, R., Nagayama, K., Ernst, R. R., & Wuthrich, K. (1981) *J. Magn. Reson.* 42, 73-87.
- Williams, T. C., Corson, D. C., & Sykes, B. D. (1984) *J. Am. Chem. Soc.* 106, 5698-5702.